AIAA JOURNAL
Vol. 36, No. 8, August 1998

Identification Approach to Estimate Buckling Load of Damaged Composite Plates

Anil L. Salunkhe* and Prasanna M. Mujumdar†
Indian Institute of Technology, Bombay 400 076, India

The application of an indirect approach for prediction of buckling loads of laminated composite plates with flaws or damage, based on the identification of the flexibility influence function of the damaged plate through experimentally measured modal vibration characteristics, is presented. The identified flexibility influence function is used in conjunction with an integral equation formulation to predict the buckling load of the damaged plate. Experiments on laminated composite plates with simulated delamination, impact damage, local step changes in thickness, and cutout have been carried out. The predicted buckling loads and modes are compared with buckling loads obtained from the actual buckling tests of these plates. The close matching between the predictions and test results shows that the lateral stiffness degradations caused by the presence of flaws and damage can be effectively captured using the identification technique.

Introduction

THE elastic stability of laminated composite structural components is an important issue in the design of modern aerospace primary structures using advanced fiber-reinforced plastic materials. During manufacture and service and due to aging and environmental effects, composite laminates are susceptible to flaws and damage such as voids, porosity, delamination, matrix cracking, fiber breakage, etc. These may not necessarily be visible or easily detectable. In critical applications, the understanding of the influence of macroscopic flaws and damage on the strength and stiffness of composite laminates forms a very important aspect of their damage-tolerant design. In the case of composite panels designed for compressive loads, such flaws and damage may cause a degradation of lateral stiffness of the panel and thus of its buckling strength. The theoretical prediction of buckling load requires a complete knowledge of the geometrical and material properties and the boundary conditions specific to the theoretical model being used. However, when some or all of these parameters are difficult to specify completely, it is difficult to predict the load theoretically. With isotropic materials, uncertainties may arise, for example, in the determination of boundary conditions. With composite materials, the uncertainties due to anisotropy, inherent nonhomogeneity, and coupling effects introduced by the laminate construction have added a dimension to the difficulty of prediction. In the presence of flaws and damage, theoretical prediction is further complicated by the need to correctly model the effect of these flaws on the lateral stiffness. Thus, in any of the aforementioned circumstances, buckling load prediction by using experimental methods may be a more reliable alternative.

A potentially attractive alternative to conventional or direct buckling tests could be an indirect route based on an identification of the effect of flaws on the lateral stiffness distribution through experimental means, followed by a computation of the buckling strength using the identified stiffness distribution. Such an indirect or a system identification approach may obviate the need for explicit knowledge of the structural properties, the modeling of the damage state, and even the need for actual loading. Some indirect methods for buckling load prediction have been investigated by earlier researchers.[1] It would be advantageous to investigate the application of these methods to damaged structures.

Presented as Paper 97-1160 at the AIAA/ASME/ASCE/AHS/ASC 38th Structures, Structural Dynamics, and Materials Conference, Kissimmee, FL, April 7–10, 1997; received Aug. 5, 1997; revision received April 8, 1998; accepted for publication April 10, 1998. Copyright © 1998 by the American Institute of Aeronautics and Astronautics, Inc. All rights reserved.

*Graduate Student, Department of Aerospace Engineering. Member AIAA.

†Associate Professor, Department of Aerospace Engineering. Member AIAA.

The aim of this study is to examine the utility of an identification approach for characterization of stiffness degradations caused by simulated flaws and damage in laminated composite plates based on measured vibration characteristics and to predict the buckling load indirectly. Natural frequencies and mode shapes of the damaged plates are determined experimentally and are then used to construct a flexibility influence function of the damaged plate. This influence function is used in an integral formulation of the buckling problem to evaluate the buckling load as an eigenvalue. The buckling load predicted by such an identification approach is compared with the critical load experimentally determined from load-deflection and strain measurements by the Southwell plot and strain bifurcation. An experimental study has been carried out on glass/epoxy plates both without and with simulated flaws. Three types of simulated damage have been considered, namely, delamination, localized impact, and local step variations in thickness.

Vibration Methods for Buckling Load Prediction

Based on the mathematical similarity between vibration and buckling, several direct and indirect methods of buckling load prediction using the measured vibration characteristics have evolved over the past few decades.[1] Buckling loads can be directly predicted from vibration frequency measurements of structures under axial loads much lower than the critical load by extrapolation on the basis of knowledge of the variation of natural frequencies with axial loads. Though theoretically justified, this method is difficult to implement in practice especially in the case of structures like plates and shells for various reasons. Foremost among them is the dissimilarity of the fundamental mode of vibration and the buckling mode.[2,3] Second, the method becomes unreliable, even in the case of columns, due to the errors in frequency measurements arising from the bending curvatures caused by the axial compressive loads.[4]

The vibration method for indirect prediction of buckling load involves determining the boundary conditions using vibration frequencies and mode shapes and then predicting the buckling load using an appropriate theoretical model. The method was first established for columns, and early work was in this direction.[5,6] Later, it was extended to stiffened shells where the effects of imperfections and eccentricities of loading were also lumped together in the boundary effects and taken into account by developing suitable theoretical models.[7] Sweet et al.[8] investigated the feasibility of the vibration method for identification of boundary conditions and prediction of buckling loads of uniform beam columns by stochastic and deterministic models. They presented a system identification theory for predicting buckling loads from vibration frequencies in terms of the rotational and translational restraints at the ends of the beam column.

A general method that predicts the buckling load of beam and plate structures with nonuniform material and stiffness properties

and with arbitrary constraints at the ends has been proposed by Baruch[9] using an integral equation formulation. The use of integral equations for formulating the buckling problem is well known and has a long history. Based on the energy approach, Baruch[9] rederived the integral equations of the buckling of beams and plates using a bending influence function and the Maxwell–Betti reciprocal theorem. In the case of plates, the integral equation can be stated as

$$w(x, y) = \iint_A \left\{ \frac{\partial K(x, y; \xi, \eta)}{\partial \xi} \left[N_x \frac{\partial w(\xi, \eta)}{\partial \xi} + N_{xy} \frac{\partial w(\xi, \eta)}{\partial \eta} \right] + \frac{\partial K(x, y; \xi, \eta)}{\partial \eta} \left[N_y \frac{\partial w(\xi, \eta)}{\partial \eta} + N_{xy} \frac{\partial w(\xi, \eta)}{\partial \xi} \right] \right\} \mathrm{d}A \qquad (1)$$

$K(x, y; \xi, \eta)$ represents the transverse deflection at (ξ, η) due to a unit force at (x, y), and $\partial K(x, y; \xi, \eta)/\partial \xi$ is the rotation at (ξ, η) due to the unit force at (x, y). By the reciprocal theorem, $\partial K(x, y; \xi, \eta)/\partial \xi$ is also the deflection at point (x, y) due to a unit moment at (ξ, η). Thus the deflection at point (x, y) due to a moment of magnitude $N_x(\xi, \eta)(\partial w/\partial \xi)\, \mathrm{d}\xi\, \mathrm{d}\eta$ arising from the applied in-plane load N_x is $[\partial K(x, y; \xi, \eta)/\partial \xi] N_x(\xi, \eta)(\partial w/\partial \xi)\, \mathrm{d}\xi\, \mathrm{d}\eta$. The integral equation is obtained by summing over the surface of the plate and including the similar terms arising from the other in-plane loads N_y and N_{xy}. The kernel of this equation is directly related to the flexibility influence function of the plate and can be found theoretically, numerically, and experimentally. Because $K(x, y; \xi, \eta)$ satisfies the boundary conditions, their explicit knowledge is not required. Once the kernel is known, the integral equation can be solved using numerical techniques to calculate the buckling load.

Using the integral equation derived for beams, Segall and Baruch[10] predicted the buckling load of elastic columns. They used the experimentally measured natural frequencies and modes to determine the influence function of the column. The results compared well with other static and dynamic tests performed on the same specimens. The method was later extended by Segall and Springer[11] to plates. The accuracy of the method was demonstrated by tests on uniform aluminum and cross-ply graphite/epoxy plates. The accuracy of the method obviously depends on the accuracy of the measured frequencies and mode shapes.

Details of the Method

In the present work, the effect of flaws and damage in laminated composite plates on their buckling loads is sought to be estimated by identification of the bending influence function. As stated earlier, Eq. (1) can be used to obtain buckling loads if the influence function is known. When the influence function is identified using experimental data, a distinct advantage of this method is that it does not require explicit modeling of the damage zone, as well as boundary conditions and material properties of the plate, nor does it require the application of axial loads.

The integral equation of buckling of a plate under uniform uniaxial loading can be written as

$$w(x, y) = \lambda \int_0^a \int_0^b \frac{\partial K(x, y; \xi, \eta)}{\partial \xi} \frac{\partial w(\xi, \eta)}{\partial \xi}\, \mathrm{d}\xi\, \mathrm{d}\eta \qquad (2)$$

where $N_x = \lambda$ is the applied load. Once the kernel $K(x, y; \xi, \eta)$ is known, Eq. (2) can be solved as an eigenvalue problem. The lowest eigenvalue of this equation is the buckling load of the plate. As pointed out earlier, the kernel of the integral equation of buckling is directly related to the flexibility influence function of the structure.

Determination of the Flexibility Influence Function

The flexibility influence function, also known as Green's function, can be obtained experimentally by measurements of static or dynamic deflections or rotations at various points on the structure due to a concentrated static or dynamic force applied one at a time at these points. However, accurate measurements of static deflections and especially rotations are difficult when they are very small.

Alternately, the influence function can be constructed from the modal vibration characteristics. With the advent of the fast Fourier transform (FFT) and advances in signal processing hardware, vibration testing of structures has become much more convenient. The kernel can be written in terms of the normal modes and vibration frequencies of the plate[12] as

$$K(x, y; \xi, \eta) = \sum_{k=1}^{\infty} \frac{\varphi_k(x, y)\varphi_k(\xi, \eta)}{\bar{M}_k \omega_k^2} \qquad (3)$$

where φ_k, $\bar{M}_k$, and ω_k are, respectively, the kth normal mode shape, generalized mass, and natural frequency of the plate. These can be measured experimentally through modal analysis, and the kernel can be approximated by a finite series of a few of the lowest modes of the structure. The accuracy of the predicted buckling loads using this approach is entirely dependent on the accuracy of the modal analysis.

Note that the effect of any variations in elastic properties due to nonuniform material distributions or geometry, the effect of actual boundary conditions, and the lateral stiffness degradations caused by the presence of a flaw or damage would automatically be taken into account in the influence function of the damaged plate through their effect on the natural frequencies, mode shapes, and generalized mass. The application of the method to the variable-stiffness situation created by the presence of damage and/or flaws has not yet been examined.

Method of Solution

The experimentally measured influence function will be known at discrete points on the plate. To solve the integral equation, a numerical approach has therefore been adopted here. Because the measurements are carried out at a limited number of points, the first step is to determine the influence function values at a larger number of points by interpolation to improve the accuracy of numerical computations. If the number of points at which the function is interpolated is r, then the influence function can be constructed as a square matrix of order $(r \times r)$. The derivative $\partial K(x, y; \xi, \eta)/\partial \xi$ is found by using the central difference scheme on the internal points and the forward and backward difference schemes at the boundary points. Similarly, the derivative $(\partial w/\partial \xi)$ can be written in terms of the values of w through these different schemes. The integral can then be evaluated by Simpson's rule.

The matrix form of Eq. (2) for a uniform compressive force $N = \lambda$ can be written as

$$\{Y\} = \lambda[\alpha]\{Y\} \qquad (4)$$

where $[\alpha] = -[\boldsymbol{S}][\boldsymbol{K}'][\boldsymbol{D}]$, where $\boldsymbol{K}'(r \times r)$ is the finite difference form of the derivative $\partial K(x, y; \xi, \eta)/\partial \xi$, $\boldsymbol{D}(r \times r)$ is the finite difference form of the operator $\partial/\partial \xi$, $\boldsymbol{S}(r \times r)$ is the weighting matrix of coefficients of Simpson's integration rule, and $\boldsymbol{Y}(r \times 1)$ is the column matrix of the deflection of the plate. The homogeneous equation (4) can be solved for the eigenvalues λ and the eigenvectors $\boldsymbol{Y}$. The lowest eigenvalue λ_{cr} will give the buckling load. If the applied external force is nonuniform, then writing $N(\xi, \eta) = \lambda p(\xi, \eta)$, where $p(\xi, \eta)$ is a known function, buckling loads can be obtained for this case also by including $p(\xi, \eta)$ in the numerical integration. The numerical algorithm and procedure for the solution of the integral equation was validated by using theoretical frequencies and mode shapes of simply supported isotropic plates and comparing the estimated load with the theoretical buckling load.

Details of the Experimental Work

The experimental work had two main components, namely, vibration and buckling experiments. In the vibration experiments, natural frequencies and mode shapes were measured by carrying out experimental modal analysis. In the buckling experiments, buckling loads were estimated by the Southwell plot based on load-deflection measurements as well as by strain measurements. The experimental setups and measurements are described briefly in the following sections. A detailed description of the experimental work is available in Ref. 4.

Support and Loading Frame for Plates

To carry out the experiments on plates, a special frame was designed to support the plate at its edges to load it in compression.

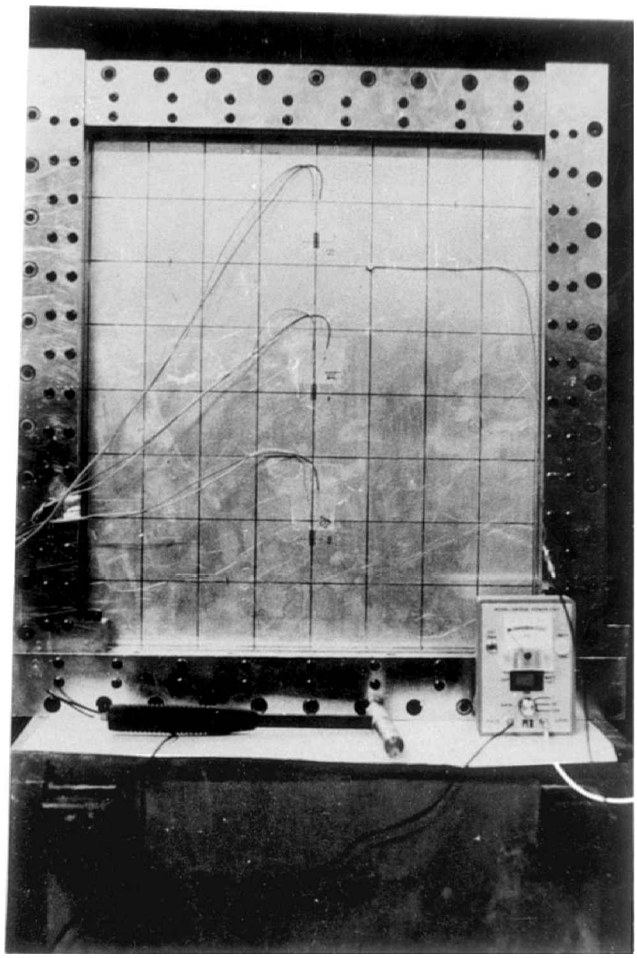

Fig. 1 Support and loading frame for plates.

Figure 1 shows the details of this rectangular frame. The vertical and horizontal posts of this frame were made as C sections to house the components that give support to the plate. These posts were made from steel bars with thick sections to make the frame mass and rigidity high compared with the plates under test and to avoid as far as possible an interaction between the modes of the plate and those of the fixture. The frame was designed so that plates of various thicknesses and aspect ratios could be accommodated. The vertical posts could be shifted along the length of the bottom channel to give three aspect ratios. The frame components were precision machined, the joints were made, and the frame was assembled to give a high accuracy on the parallelism of the vertical and horizontal posts with no looseness. The upper horizontal post moved smoothly inside the vertical supports.

Laminates of length 470–520 mm and width 420, 320, and 200 mm can be clamped in the frame using bars of rectangular cross section of 30-mm width, placed on either side of the plate inside the C section of the posts. The clamping pressure was provided by the twin set of screws on each flange of the C posts. To maintain adequate and uniform pressure over the full length of each plate, a large number of screws at close intervals were provided. Teflon® tapes were inserted between the plate specimen and the clamping bars to reduce friction so that the specimen is uniformly loaded. Plates of thickness 1–5 mm can be clamped in the C posts of the fixture.

Experimental Modal Analysis

The impulse response technique was used for modal analysis of plate structures. The modal analysis was based on measurements of the accelerance transfer function through impact excitation and acceleration response measurements. The impact excitation was given by a PCB Series 291B modally tuned impact hammer. The acceleration response was measured by a B&K Type 8307 miniature accelerometer (mass less than 1 g) to minimize mass loading. Signal conditioning of the impulse force and acceleration signals was achieved by using a PCB 480D06 voltage amplifier and a B&K Type 2635 charge amplifier, respectively. The force and acceleration signals were input to the Iwatsu SM-2701 dual-channel FFT analyzer for transfer function analysis.

Because the work involved extensive modal analysis experiments, the FFT analyzer was linked to a personal computer through an IEEE-488 interface card, and control programs were written for operation, front panel settings, and data transfer. An interactive modal analysis software program was written to automatically control the modal analysis experiment with user inputs taken for setting the parameters and postprocessing the measured frequency response functions by the single-degree-of-freedom (SDOF) circle fit method and computing the natural frequencies and mode shapes from these data. The system, software, and procedure for modal analysis were validated through initial experiments on uniform isotropic free-free plates and cantilever beams by comparison with theoretical results.

Specimen Preparation

The plate specimens were made from glass/epoxy composite material. Laminates were made from plain-weave glass fabric (7 mil) and epoxy resin CIBA LY556 with hardener HT972 using room-temperature curing, which generally resulted in laminates with volume fractions in the range of 33–47%. A few laminates were also made using high-temperature curing (with hardener HT951), which allowed a better squeezing out of excess resin, resulting in higher volume fractions (55–60%). Thickness variations from 5–10% were present in each cured laminate. For a laminate made using N number of fabric layers oriented such that the warp and fill directions were parallel to the plate edges, the resulting layup could be taken to be equivalent to $[0/90]_N$. The laminates were inspected using backlighting for any visible large flaws, such as voids. While fabricating the test specimens, the plate edges were carefully machined by milling so that the two opposite edges were parallel to each other. Table 1 describes the specimen in terms of its layup, its dimensions, and the type of simulated damage. Some plate specimens were also fabricated without introducing any flaw or damage. In Table 1, the notation P is used for plates without flaws and/or damage, and the notation DP is used for plates with simulated flaws and/or damage. The variation of thickness in different laminates with the same number of layers, seen in Table 1, was because of the difference in the fabrication methods used, resulting in different volume fractions as described earlier. The same reason explains the comparatively lower thickness of the 16-layer laminates.

Three types of flaws and/or damage were simulated in the test specimens. The first was delamination. The plate specimen DP1 was made by embedding a thin Teflon film between the layers at the time of layup of the laminate. The size of the central midplane delamination introduced into DP1 was about 20% of the plate test area. The second type of flaw was simulated by impacting the laminates. The specimen DP2 was made by impacting the plate P3 using a guided drop-weight impact testing machine with a conical impactor producing localized damage. However, the impactor at its maximum energy produced only a small region of localized surface damage around the contact point. To obtain an impact damage distributed over a larger region of the plate, a setup along with a steel ball as the impactor was used. The steel ball, which was 3 in. in diameter and weighed around 2 kg, was dropped from a height of 3 m on the plate DP3 at four close locations around its center to produce an overall damage zone of area 75 × 75 mm, i.e., about 4% of the plate area. To reduce the plate bending during the impact, the plate specimen DP3 was clamped around a small area (5 × 5 in.) of the plate. Debonding and fiber breakage were observed in the lowermost layers as a result of the impacts.

The third type of damage considered in this work was an idealized form in which the material from a part of the plate was removed by machining, giving rise to a step change in thickness. It represents the case in which the material in the damaged region is assumed to be totally ineffective in load transfer and stiffness contribution, such as in the case of localized extensive matrix cracking and fiber breakage in some layers. Three specimens—DP4, DP5, and DP6—were fabricated in this category. After the experiments on the impacted specimen DP3 were completed, a cutout of about 5% of the area (86 × 80 mm) at the center of the plate was made by machining

Table 1 Description of the plate test specimens

Plate	Layup	Dimensions, mm	Simulated damage	
			Type	Description
P1	Aluminum	$410 \times 360 \times 1.60$	——	——
P2	$[0/90]_{12}$	$410 \times 360 \times 2.08$	——	——
P3	$[0/90]_{16}$	$390 \times 260 \times 2.47$	——	——
P4	$[\pm 45]_{12}$	$410 \times 360 \times 2.41$	——	——
DP1	$[0/90]_{12}$	$410 \times 360 \times 2.91$	Delamination	Central, midplane delamination of 20% plate area
DP2	$[0/90]_{16}$	$390 \times 260 \times 2.47$	Impact	Central localized impact using conical impactor
DP3	$[0/90]_{12}$	$410 \times 360 \times 2.53$	Impact	Central distributed impact using steel ball impactor over 4% area
DP4	$[0/90]_{12}$	$410 \times 360 \times 2.53$	Cutout	Central rectangular cutout of 5% area
DP5	$[0/90]_{22}$	$410 \times 360 \times 3.56$	Stepped	Material removed from one surface over 22% area at plate center
DP6	$[0/90]_{22}$	$410 \times 360 \times 3.56$	Stepped	Material removed from both surfaces over 27% area at plate center
DP7	$[0/90]_{8}$	$410 \times 360 \times 1.73$	Drop ply	——
	$[0/90]_{12}$	$410 \times 360 \times 2.64$		

out the impact damage zone. The resulting plate specimen was termed DP4. In the case of DP5, a 27% step change in thickness was produced by machining out a few layers over a central area of 235×140 mm (22% of the area of the plate). This resulted in a sudden drop in the lateral stiffness over the central area, inducing bending and stretching coupling. After the vibration and buckling experiments were completed on DP5, the same plate was used to prepare DP6 by removing the material on the other surface of DP5 such that a total thickness reduction of about 60% was symmetrically produced over the central area of 235×170 mm.

A step variation in the lateral stiffness was also simulated without machining of the plate by dropping plies during layup (specimen DP7). The basic plate was a symmetric cross-ply laminate with a total of 12 layers. Four layers at the midplane of the laminate were dropped at the centerline perpendicular to the loading direction, resulting in a $[0/90]_8$ laminate in one-half of the plate.

Vibration Experiments

A fixed impulse location (usually close to the clamped end or corner) and a variable accelerometer position were used in all of the experiments. Around 49–81 points were selected in the form of a rectangular mesh on the plate surfaces for vibration measurements. An odd number of grid lines along the x and y directions were selected to ensure the measurements of node and antinode occurring at the centerlines of the plate. The measurement mesh was chosen to be finer near the edges than at the center. About 10–12 modes were included in the modal analysis, which in most cases covered a range of 1 kHz. The measurements in this range were usually carried out at all points over more than one frequency band using the zoom facility of the FFT analyzer to improve accuracy, especially in the case of modes with close frequencies. Vinyl tips were used in the low-frequency range up to 200 Hz, and a Teflon tip was used in the higher range up to 1000 Hz.

A summation averaging was used in the transfer function measurement to remove noise. The number of averages was chosen such that the transfer function was adequately smooth around a resonance. This was alternately monitored by the coherence function value around the resonances; the frequency response functions with coherence above 0.9 were accepted. The transfer function data were processed by the SDOF circle fit method for obtaining the natural frequencies and mode shapes. This was found to be accurate enough for the type of plate structures tested.

Buckling Experiments

All of the buckling tests were carried out under position control mode on the Instron 8500 universal testing machine. Figure 2 shows the experimental setup. The plate specimen DP1 with delamination

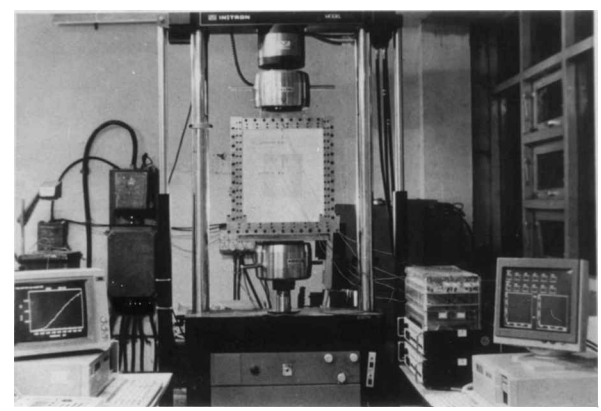

Fig. 2 Experimental setup for plate buckling tests.

can also be seen clamped in the support and loading frame in Fig. 2. Measurements were made of the transverse and axial displacements and strains at various loads. Transverse deflections were measured using dial gauges with 0.01-mm accuracy that were located at three points along the centerline in the loading direction (x direction). Back-to-back strain gauges were also bonded at these locations. At each location, two strain gauges of 350 Ω were attached on each surface, one in the loading direction and the other transverse to it. In the first few plates, additional strain gauges were placed along the top edge to check the uniformity of the applied load along the y direction. A personal-computer-based strain measurement system with 15 quarter-bridge strain channels and 1 load channel was used. Each quarter-bridge was itself constructed from 350-Ω strain gauges mounted on a thick glass/epoxy plate for temperature compensation. From the measured back-to-back strains at each load, axial and bending strains at each location were determined.

Results and Discussion

Table 2 shows the buckling loads predicted by the identification approach along with the buckling loads obtained experimentally from the measured load-strain and load-transverse deflection data using the strain bifurcation and Southwell plot method. All plate specimens, except P3 and DP2, were tested with all edges clamped. In the case of P3 and DP2, the unloaded edges were free. Theoretical estimates of the buckling loads are also reported for comparison in the case of plates without flaws. In the case of the plates with flaws, the theoretical loads in the last column of Table 2 indicate the buckling loads, assuming that no damage is present. These have been given to indicate the extent of loss of buckling strength caused by

Table 2 Comparison of plate buckling loads obtained by various methods

Plate specimen	Strain bifurcation load, kN	Southwell plot method		Identification approach		Theoretical[a] estimate, finite element method	
		Load, kN	Mode	Load, kN	Mode	Load, kN	Mode
P1	7.3	7.1	1	7.3	1	7.2	1
P2	4.3	4.3	2	4.2	2	4.2	1
P3[b]	2.1	2.5	1	2.2	1	2.3	1
P4	5.5	5.8	2	5.8	2	5.5	2
DP1	9.0	9.5	2	9.3	2	8.4	2
DP2[b]	2.3	2.2	1	2.3	1	2.3	1
DP3	4.8	5.0	2	4.9	2	6.2	2
DP4	4.7	4.3	2	4.3	2	6.2	2
DP5	15.8	14.9	1	15.9	1	22.1	2
DP6	7.3	7.5	2	7.6	2	22.1	2
DP7	1.9	2.1	1	2.0	1	1.9	1

[a]Theoretical buckling load (and mode) of corresponding undamaged plate is given in case of plate with flaws or damage.
[b]Tested in C-F-C-F configuration.

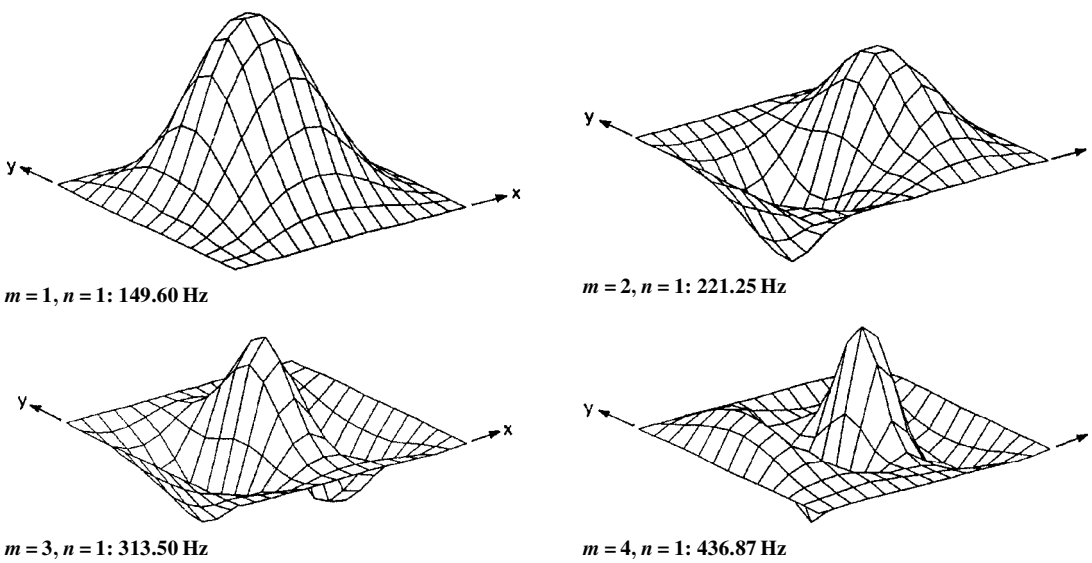

Fig. 3 Measured vibration mode shapes of plate DP6.

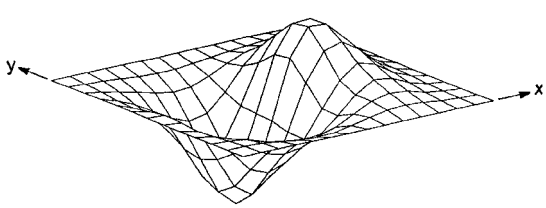

Fig. 4 Predicted buckling mode shape of plate DP6.

the flaw and/or damage. The theoretical estimates were obtained by finite element analysis using the SHELL99 element of ANSYS(5.3).

In describing the mode shapes of buckling in Table 2, mode 1 refers to a deformation shape with predominantly one half-wave in each direction ($m = 1$ and $n = 1$), and mode 2 refers to the shape with predominantly two half-waves in the loading direction and one in the unloaded direction ($m = 2$ and $n = 1$).

Figures 3–7 depict a few typical results of the modal measurements and buckling tests carried out, from which the buckling loads given in Table 2 are derived. Further details and experimental results for all specimens tested are available in Ref. 4.

Plates Without Flaws or Damage

Initially, experiments were conducted on uniform plates (without any flaw or damage) to establish the accuracy of the prediction and the confidence in the application of the identification technique as well as to determine the number of vibration modes required. Because only uniaxial loading was considered in this study, it was obvious that the buckling mode could not have nodal lines along the x direction. Thus, it was necessary to use only vibration modes with one half-wave in the y direction, i.e., modes with $n = 1$, to construct the influence function in the identification approach.

A convergence study was carried out by using an increasing number of measured modes ($m = 1$–4 and $n = 1$) to reconstruct the flexibility influence function. The convergence study showed that the use of more than three modes did not further improve the accuracy in the estimation of the buckling load significantly. It can be seen from Table 2 that the buckling load thus predicted compares very well with the actual load obtained experimentally, as well as the purely theoretical estimates, for all uniform plate specimens P1–P4.

A close examination of the predicted buckling mode showed that it was not symmetrical along the loading direction. This was because the upper edge of the plate, which is also the loading edge, is not fully constrained, as it has to have in-plane freedom to compress the plate. To allow smooth movement of the upper horizontal post of the fixture inside the vertical posts, small gaps have to be provided. This means that the upper edge is not perfectly clamped. This causes the asymmetry in the loading direction. This asymmetry was also evident during the buckling tests from the transverse displacement measurements. Thus, the predicted and the observed modes matched well.

Plates with Flaws or Damage

A comparison of the buckling loads of the plates with flaws and/or damage (DP1–DP7) in Table 2 also shows a very good correlation between the value predicted by the identification approach and the actual loads obtained through direct tests. Three vibration modes were used to construct the flexibility influence function. In most

of the cases, although the experimental modal measurements were carried out at around 81 points (9×9 grid), the computation of the buckling load using Eq. (4) was carried out on an extended grid of 15×13 points through interpolation of the mode shapes. As a typical example, Fig. 3 shows some of the measured vibration modes of the plate DP6 along with their frequencies. In comparison with the mode shapes of uniform plates of the same size and material, the modal slopes were seen to be relatively higher at and around the center due to the flexible thinner section when the mode shapes were normalized with respect to the maximum displacement.

The buckling mode estimated form Eq. (4) for this plate is mode 2 as shown in Fig. 4, with a critical load of 7.6 kN, which matches with the load of 7.3 kN given by the strain bifurcation in the plots as shown in Figs. 5a–5c. Figure 5d shows the Southwell plot based on the measured bending strain data obtained from the back-to-back strain gauges at the plate center, which gives the buckling load as 7.5 kN, which also compares well. Comparing this with the theoretical estimate of the buckling load (22.1 kN) of the parent plate (without considering the step reduction in thickness), the reduction in buckling load is about 66%, and this drop has been well predicted by the identification approach.

In contrast to DP6, which has a symmetrical step reduction in thickness, plate DP5, which has an asymmetrical step reduction in thickness, buckles in the mode shown in Fig. 6. This asymmetry in DP5 clearly causes the load plane to be eccentrically placed with respect to the thinner section of this plate, thereby causing larger displacements and bending strains at low load levels in this plate in a predominantly mode 1 type of deformation. This is evident from Figs. 7a–7d, which show the load-strain and load-transverse deflection plots. This eccentricity thus causes the plate to tend to buckle in mode 1, even though the corresponding parent laminate without the step reduction in thickness would buckle in mode 2 as predicted theoretically. As a result, the buckling mode of DP5 is intermediate between mode 1 and mode 2 deformations as shown in Fig. 6. The predicted and actual buckling loads match well and show a drop of about 28% with respect to the undamaged laminate.

The buckling load of the plate with delamination (DP1) does not show any significant change due to the flaws when compared with the buckling load of the corresponding undamaged plate. Thus, even a 20% central midplane delamination does not seem to affect the lateral stiffness, and this is correctly reflected in the predicted buckling load. In fact, the measured natural frequencies of the delaminated plate, given in Table 3, do not show much difference with respect to the theoretical natural frequencies of the corresponding plate (parent) without delamination. Differences very similar to those in Table 3 are also obtained when measured natural frequencies of the aluminium plate (P1) are compared with theoretical estimates, showing that these differences were due to the experimental conditions.

Similarly, a highly localized impact damage (plate DP2) does not affect the buckling load. However, plate DP3 with the distributed impact damage shows a 21% drop in the buckling load, which is accurately predicted by the identification method. A comparison of the buckling load of plate DP4 with that of DP3 gives an assessment of the implication of modeling such an impact damage by replacing the damage zone by a hole, i.e., assuming the damage zone has effectively no contribution to the lateral stiffness. The buckling load of DP4 is not seen to be very different from that of DP3, showing that such a simplified approach may have some justification.

Table 3 Comparison of natural frequencies in hertz of plate with delamination (DP1) and the corresponding plate without delamination

	$n = 1$		$n = 2$	
m	Parent	DP1	Parent	DP1
1	103.35	109.10	230.23	243.75
2	193.82	182.32	297.62	312.50
3	346.61	304.86	429.88	428.15

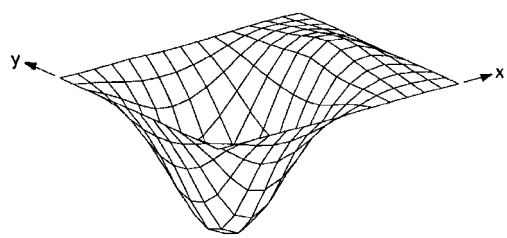

Fig. 6 Predicted buckling mode shape of plate DP5.

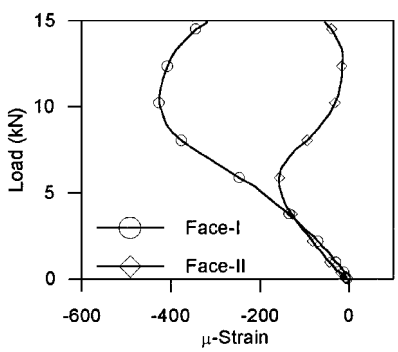

a) Back-to-back strains at center

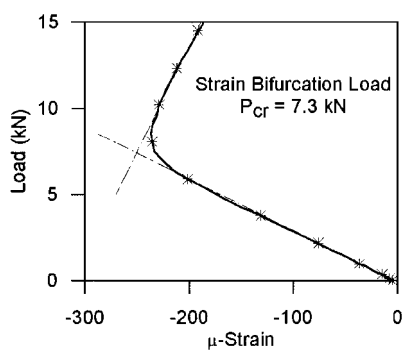

c) Strain bifurcation plot using axial strain

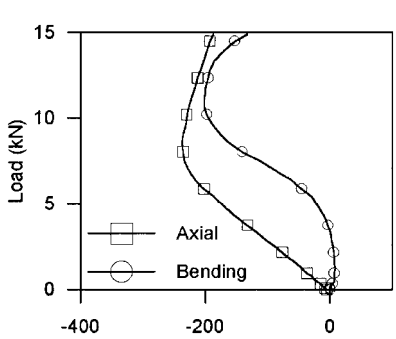

b) Axial and bending strains at center

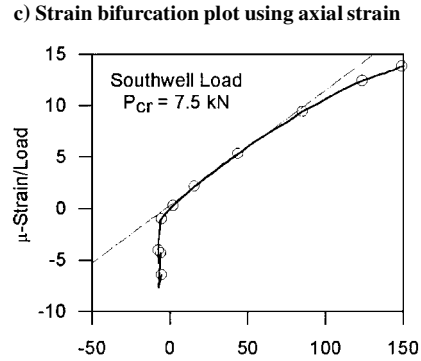

d) Southwell plot using bending strain

Fig. 5 Buckling test results of plate DP6.

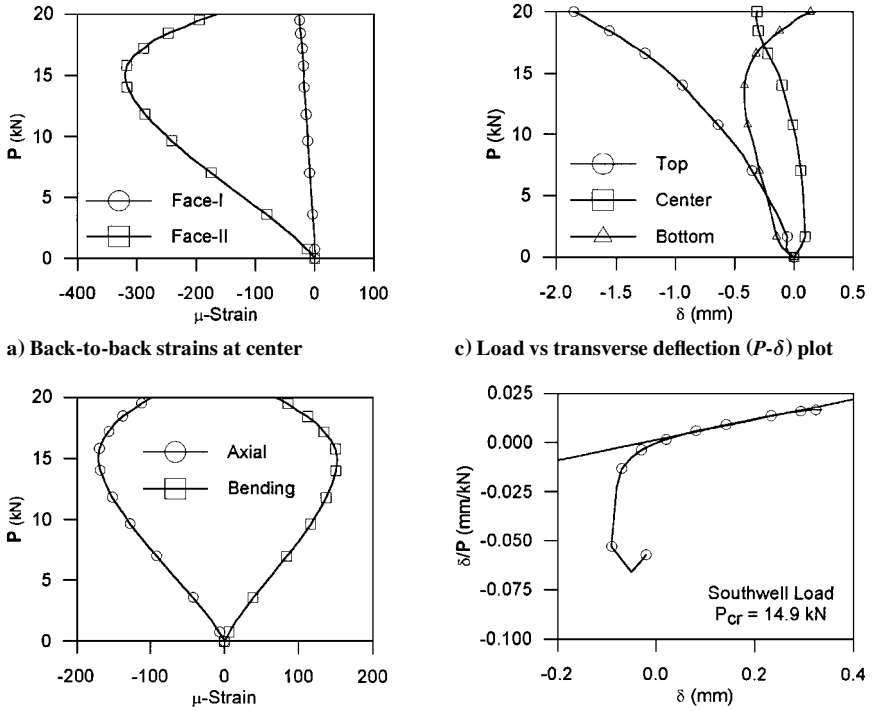

a) Back-to-back strains at center

c) Load vs transverse deflection (P-δ) plot

b) Axial and bending strains at center

d) Southwell plot using transverse deflection at the center

Fig. 7 Buckling test results of plate DP5.

Concluding Remarks

A system identification approach to predict buckling loads of composite laminates with flaw and/or damage, based on the reconstruction of a flexibility influence coefficient matrix of the damaged laminate from experimentally measured natural frequencies and mode shapes, is examined. The extensive experiments conducted clearly show that the reconstruction of the flexibility influence coefficients can be accurately carried out through measured modal vibration characteristics even under the conditions of abrupt variation in stiffness such as those resulting from impact damage, cutout, local step changes in thickness, ply drop, and delamination. The investigations also show that the reduction in buckling load caused by the damage can be accurately estimated by this approach. This has important implications where the theoretical modeling of laminates with such and other damage may be difficult. In such cases, the identification of the model from experimental measurements may provide a good alternative.

References

[1]Mujumdar, P. M., and Suryanarayan, S., "Nondestructive Techniques for Prediction of Buckling Loads—A Review," *Journal of the Aeronautical Society of India*, Vol. 41, No. 2, 1989, pp. 205–223.

[2]Jub, J. E. M., Phillips, I. G., and Becker, H., "Interrelation of Structural Stability, Stiffness, Residual Stress and Natural Frequency," *Journal of Sound and Vibration*, Vol. 39, No. 1, 1975, pp. 121–134.

[3]Abramovich, H., "Correlation Between Vibration and Buckling of Stiffened Cylindrical Shells Under External Pressure and Combined Loading," *Israel Journal of Technology*, Vol. 16, No. 1–2, 1978, pp. 34–44.

[4]Salunkhe, A. L., and Mujumdar, P. M., "Estimation of Buckling Loads of Damaged Composite Laminates by Nondestructive Dynamic Methods," Dept. of Aerospace Engineering, Indian Inst. of Technology, TR ARDB-SP-TR-1994-639-02, Bombay, India, Feb. 1994.

[5]Klien, B., "Determination of Effective End Fixity of Columns with Unequal Rotational End Restraint by Means of Vibration Test Data," *Journal of the Royal Aeronautical Society*, Vol. 61, Feb. 1957, pp. 131, 132.

[6]Jacobson, M. J., and Wenner, M. L., "Predicting Buckling Loads from Vibration Data," *Experimental Mechanics*, Vol. 8, No. 10, 1968, pp. 35N–38N.

[7]Singer, J., "Vibration Correlation Techniques for Improved Buckling Predictions of Imperfect Stiffened Shells," *Buckling of Shells in Offshore Structures*, Granada Publishing, New York, 1982, pp. 285–330.

[8]Sweet, A. L., Genin, J., and Mlakar, P. F., "Determination of Column Buckling Criteria Using Vibration Data," *Experimental Mechanics*, Vol. 17, No. 10, 1977, pp. 385–391.

[9]Baruch, M., "Integral Equations for Nondestructive Determination of Buckling Loads for Elastic Bars and Plates," *Israel Journal of Technology*, Vol. 11, No. 1–2, 1973, pp. 1–8.

[10]Segall, A., and Baruch, M., "A Nondestructive Dynamic Method for the Determination of the Critical Load of Elastic Columns," *Experimental Mechanics*, Vol. 20, No. 8, 1980, pp. 285–288.

[11]Segall, A., and Springer, G. S., "A Dynamic Method for Measuring the Critical Loads of Elastic Flat Plates," *Experimental Mechanics*, Vol. 26, No. 4, 1986, pp. 354–359.

[12]Bisplinghoff, R. L., Ashley, H., and Hoffman, R. L., *Aeroelasticity*, Addison–Wesley, Reading, MA, 1955, pp. 87–95.

A. Berman
Associate Editor